Band structure in ^{180}Re and the different coupling schemes in a deformed doubly odd nucleus

A. J. Kreiner
Departamento de Física, Comisión Nacional de Energía Atómica, 1429 Buenos Aires, Argentina and Brookhaven National Laboratory, Upton, New York 11973

J. Davidson, M. Davidson, D. Abriola, and C. Pomar
Departamento de Física, Comisión Nacional de Energía Atómica, 1429 Buenos Aires, Argentina

P. Thieberger
Brookhaven National Laboratory, Upton, New York 11973

(Received 26 May 1987)

Rotational bands in the odd-odd nucleus ^{180}Re have been studied via the ^{176}Yb(^{10}B,6n) and ^{181}Ta(α,5n) fusion-evaporation reactions. A completely new high-spin level scheme has been obtained comprising four $\Delta I=1$ bands and a $\Delta I=2$ band. The $\Delta I=1$ structures can be understood from quasiparticle states in neighboring odd nuclei and the $\Delta I=2$ band is interpreted as a new example of a double decoupled sequence based on the decoupled $h_{9/2}$ proton and a $\frac{1}{2}^-[521]$ neutron. The different coupling schemes in a deformed doubly odd nucleus are discussed.

I. INTRODUCTION

^{180}Re has been studied as a part of a continued effort[1] to obtain information on collective and single particle phenomena in doubly odd nuclei. Prior to this work only a few low spin states, populated through the electron capture decay of ^{180}Os, were known in ^{180}Re (Ref. 2). In particular, the $(1)^-$, 2.4 min ground state and a $(1)^+$ excited state at 20.2 keV were established. The part of the spectrum populated in the present work has no states in common with the previously known one and it must be built on a hitherto unknown isomer at rather low excitation energy.

In the course of the present investigation information was also obtained on ^{182}Re which corroborates recently published data.[3]

II. EXPERIMENTS

A self-supporting, ≈ 5.5 mg/cm^2 thick foil of enriched ($\approx 97\%$) ^{176}Yb was the target for the ^{176}Yb(^{10}B,xn) reaction. The ^{10}B beam was delivered by the Brookhaven National Laboratory MP7 tandem and an excitation function was measured comprising the energies 45, 50, 55, 60, 65, 70, and 73 MeV. As a crosscheck, the reaction ^{181}Ta(α,5n)^{180}Re was measured at 55 MeV bombarding energy at the Buenos Aires Synchrocyclotron.

A. Singles γ-ray spectra

Singles γ-ray spectra were taken with a Ge(Li) detector surrounded by a large NaI Compton suppressor annulus. (Such a setup is well known nowadays to be crucial for detailed spectroscopy in complex nuclei.) Figure 1 shows such a γ-ray spectrum at $E(^{10}\text{B})=73$ MeV and 90° to the beam direction. It is indeed a very complex spectrum. At 73 MeV the excitation energy of the compound nucleus is rather high and the number of open channels is large. There is evidence at this bombarding energy of in beam production of $^{179-181}$Re (7n,6n,5n) (Refs. 2 and 4), $^{179-181}$W (p6n,p5n,p4n) (Ref. 2), and $^{177-178}$Ta (through α5n and α4n reactions, respectively) (Refs. 2 and 5). The isotopic assignment of lines to ^{180}Re was done on the basis of excitation functions, prior knowledge of neighboring nuclei (in particular, ^{179,181}Re) (Refs. 2 and 4), and coincidences with Re x rays. The study of the subsequent decay of ^{180}Re to ^{180}W shows complete agreement with the published data.[2]

One concludes that the population of ^{180}Re goes through its known $(1)^-$ ground state. Table I gives γ-ray energies, γ-ray and total transition intensities, and a_2 angular distribution coefficients for the cases where a value could be extracted.

B. Coincidence measurements

Conventional three parameter E_{γ_1}-E_{γ_2}-$t_{\gamma_1\gamma_2}$ coincidence data were taken, using on one side of the target (90° and ≈ 10 cm distance to the beam) the Compton suppressed Ge(Li) detector and on the other (90° and ≈ 2 cm) an intrinsic Ge counter of $\approx 15\%$ efficiency, and stored event by event on magnetic tape. Extensive off-line sorting of these data enabled us to construct a rather complex and completely new level scheme to be discussed in the next section. Figures 2–4 show illustrative gated spectra. Figures 2 and 3 correspond to gates set both on the energy of a certain γ ray (as indicated) and the time dimension [the inset on each spectrum shows qualitatively the location of the time window on a symbolic time to amplitude converter (TAC) curve]. The

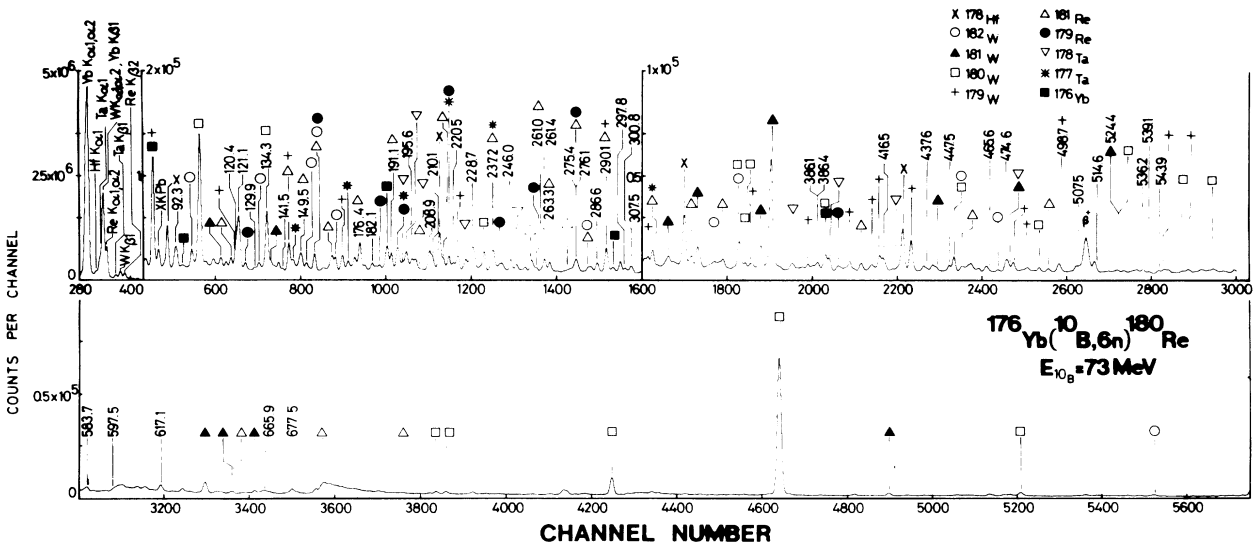

FIG. 1. Singles γ-ray spectrum from the ^{176}Yb(^{10}B,xnyp$z\alpha$) reaction. Lines labeled by their energies are identified as transitions in ^{180}Re.

TAC range was 400 ns and the prompt curve (full width at half maximum $\approx$15 ns) was placed symmetrically using a 200 ns delay between start and stop detector. Since the start signals were derived from the gating detector a window on the left-hand (right-hand) side of the prompt TAC curve means events in the displayed detector coming "early" ("late") with respect to the gating γ ray. For instance, at the bottom of Fig. 2 we see that the 120.4 and 134.3 keV (also 263.3 and 276.1 keV) lines temporally precede the 246.0 keV gating line. Displaying the time distributions (TAC curves) of particular γ rays against the others led to the establishment of three different isomeric levels (see next section). Figure 4 corresponds to three gated spectra with no further timing requirement (i.e., the full range of 400 ns in the TAC is accepted), since there is no lifetime involved in the cascade to which these γ rays belong. Random coincidences, monitored through the target x-ray intensity, which is very large in singles, were negligible.

III. LEVEL SCHEME

The completely new level scheme obtained in the present work is shown in Fig. 5. There is no overlap or connection between the transitions identified here and the few previously known low spin states. Since our decay measurements coincide with the published data[2] for the $(1)^-$ ground state, we are forced to think that our "effective" (5^+) ground state (see below) cascades down through possibly highly converted (and perhaps isomeric) low energy transitions. Its excitation energy remains undetermined (<150 keV).

The level scheme of Fig. 5 follows from a joint consideration of all the available information, which includes singles γ-ray intensities, angular distributions, and a careful quantitative evaluation of coincidence intensities (prompt as well as delayed).

The new level scheme proposed in the present work comprises four $\Delta I=1$ cascades and a $\Delta I=2$ cascade. Since there is no direct information about the state on which the whole scheme is built, the assignment of spin parities appears to be a difficult task which will have to rely on more theoretical considerations (see next section). Here we shall restrict ourselves to the construction of the scheme from the mutual relations among the states as implied by the experimental information.

We shall start discussing the band at the right-hand side of Fig. 5, which starts at 259.7 keV.

Gates on one of the strongest members of this band (B band), i.e., the 176.4 keV γ ray, are shown in Fig. 2. The prompt coincidences (top spectrum) show mainly the upper members of the band [i.e., 210.1, 237.2, 261.0, 282.5, and 300.8 keV ($\Delta I=1$) and the crossover 447.5, 498.7, 543.9, and 583.7 keV transitions]. There is, in addition, the strong 134.3 keV line in prompt coincidence with the gating transition which possibly is the first member of this cascade. Additional evidence to support this association comes from the existence of the weak 311.0 keV crossover (134.3 + 176.4=310.7 keV). [However, there is an alternative interpretation which is, as will become clear in the next section, also consistent with the picture of ^{180}Re we shall construct. Namely, there is an $I^\pi=9^-$ band in ^{182}Re (see Fig. 6 of Ref. 3) which is very similar to the portion of the B band starting at 394.0 keV. Both the $\Delta I=1$ as well as the $\Delta I=2$ crossover transitions are indeed very similar in energy for both nuclei, suggesting equal structure.] This gate (the 134.3 keV) is contaminated with the 177.1 keV line of ^{181}Re (Ref. 4), which accounts for the 118.1, 148.5, and 202.7 keV transitions. [Incidentally, it is worth mentioning that the time calibration was checked with the 144.7 keV line of $T_{1/2}=156$ ns in ^{181}Re (Ref. 4).] The second spectrum from above in Fig. 2 shows three

lines which come temporally after the gate, namely the 78.6, 92.3, and 121.1 keV γ rays. This clearly defines an isomeric level in between. It turns out that the isomeric transitions are the 78.6 and the 121.1 keV lines, which depopulate a state of $T_{1/2}=78\pm9$ ns. [That the proper ordering for the 121.1 and 92.3 keV lines is the one shown is substantiated by the prompt coincidence between the 92.3 keV line and others (like the 246.0 keV

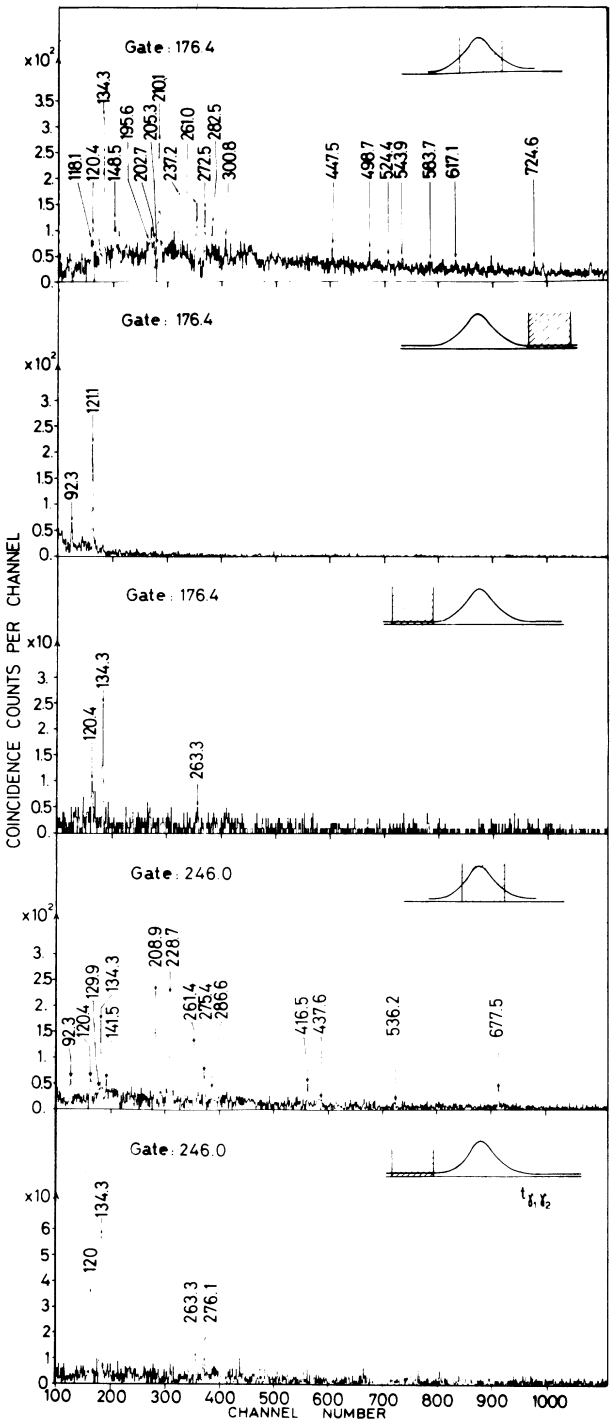

FIG. 2. Coincidence spectra gated by the 176.4 and 246.0 keV transitions. The top and second from below spectra correspond to prompt coincidences. Time gates were set on the TAC curves as indicated by the dashed windows. Windows to the left (right) of the prompt curve correspond to events coming "early" ("late") with respect to the gating transition.

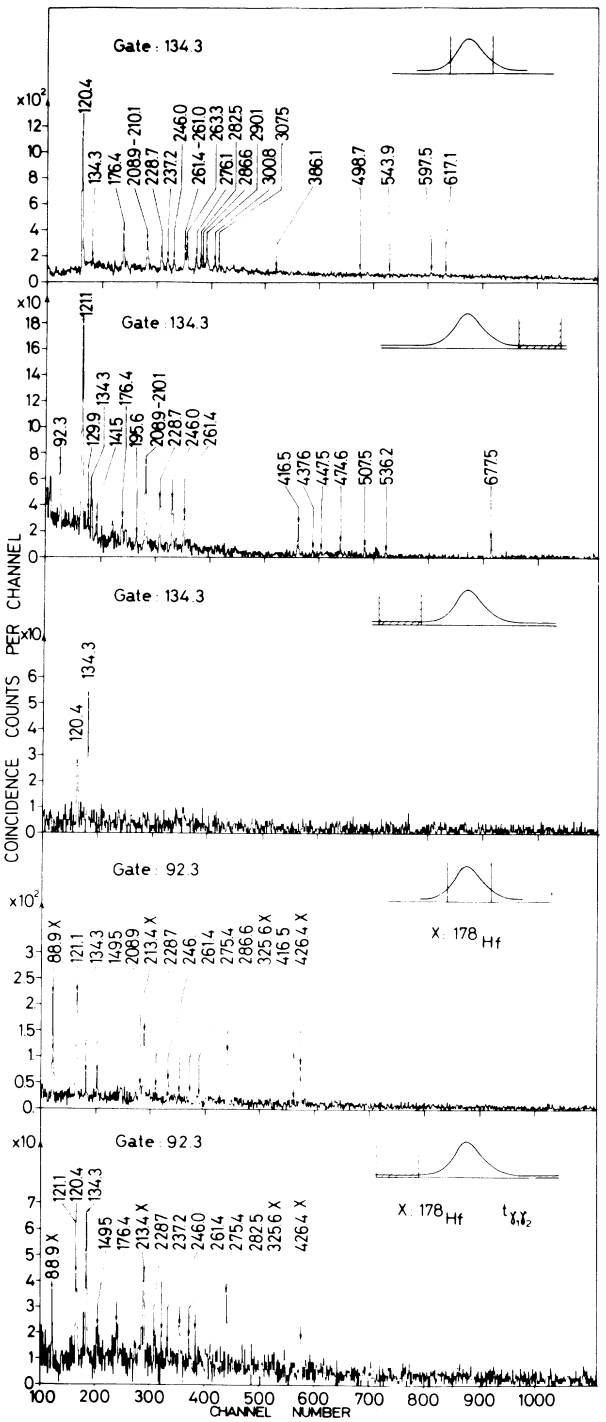

FIG. 3. Coincidence spectra gated by the 134.3 and 92.3 keV transitions corresponding to various timing conditions. $\times$ denotes transitions in ^{178}Hf. They appear because the 92.3 keV gate comprises the 93.2 keV, $2^+\rightarrow0^+$ transition in ^{178}Hf coming from the decay of ^{178}Ta.

TABLE I. γ-ray energies[a] and intensities, total transition intensities according to assigned multipolarity (see text), and angular distribution coefficient a_2 for ^{180}Re from the ^{176}Yb(^{10}B,6n) reaction at 73 MeV.

E_γ (keV)	I_γ (arb. units)	I_T (arb. units)	Multipolarity	a_2
42.3	36(7)	56(11)	$M1$	
46.3	50(25)	76(38)	$M1$	
78.6	33(4)	6(1)	$E1$	
92.3[b]	100(10)	100(10)	$M1$	−0.7(2)
120.4	118(20)	18(3)	$E1$	D[d]
121.1	319(44)	50(7)	$E1$	D
134.3[f]	92(13)[e]	40(6)	$M1$	D
134.3[g]	176(27)[e]	26(4)	$E1$	
134.3	81(12)[e]	26(4)	$E2$	
141.5	8(2)	1.2(2)	$E1$	
149.5	61(12)	21(4)	$M1$	−0.4(2)
176.4	134(22)	37(6)	$M1$	
182.1	43(4)	11(1)	$M1$	
191.1[c]	44(13)	7(2)	$E2$	
208.9	127(19)	27(4)	$M1$	D
210.1	105(14)	22(3)	$M1$	−0.31(16)
220.5	18(4)	3.6(8)	$M1$	
228.7	96(16)	18(3)	$M1$	−0.3(1)
237.2	62(10)	11(2)	$M1$	
237.6[h]	<25	<3		
246.0	85(8)	15(2)	$M1$	
261.0[e]	47(6)[e]	8(1)	$M1$	
261.4[e]	58(9)[e]	10(2)	$M1$	
263.3	58(11)	10(2)	$M1$	
275.4[e]	38(8)[e]	6(1)	$M1$	D
276.1[e]	50(13)[e]	8(2)	$M1$	
282.5	36(7)	6(1)	$M1$	
286.6	27(6)	3.5(7)		
290.1	38(8)	6(1)	$M1$	D

line; see second spectrum from below in Fig. 2).]

The third spectrum from above in Fig. 2 shows that there are also lines which temporally precede the 176.4 keV transition, indicating the existence of a second isomeric state feeding into this band.

There is another cascade (A band) in parallel to the one discussed above and which is based on a state at 180.9 keV. A representative member is the 246.0 keV transition, and we show two spectra gated by this line with two different temporal conditions. The prompt spectrum shows mainly the band members (this *band* character is underlined by the presence of all the crossover transitions, the smoothly increasing transition energy, and the angular distribution data): 208.9, 228.7, 261.4, and 275.4 keV lines ($\Delta I = 1$), and out of band transitions (mainly 677.5, 416.5, and 141.5 keV lines) connecting this structure with the higher lying isomeric state. The transitions feeding this isomeric state (at 1542.1 keV) are again seen in the bottom spectrum of Fig. 2. These include prominently a 134.3 keV γ ray. The establishment of the present level scheme was considerably complicated by the fact that the 134.3 keV line is triple (and unresolved within our experimental energy resolution). That there are at least two lines of 134.3 keV is clearly shown in the third spectrum from above in Fig. 3. The 134.3 keV line shows up in a spectrum gated by its very same energy. An indication of the third 134.3 keV transition comes from a quantitative consideration of the intensity of this γ ray in prompt and delayed coincidence with the members of the A band. There is systematically more intensity of the 134.3 keV γ ray in the prompt gate than in the gates with the TAC window on the left-hand side of the prompt curve (events coming "early") (compare the two gates in coincidence with the 246.0 keV line on Fig. 2). In addition, there is a 42.3 keV γ ray in prompt coincidence with the members of the A band and with the 92.3 keV line. In fact, the third 134.3 keV line is the crossover for the 42.3 and 92.3 keV transitions.

The second spectrum from above in Fig. 3 shows again that the upper lying isomer feeds both A (more strongly) and B bands. The lifetime of the isomer is determined to be 67±9 ns.

The spectrum in prompt coincidence with the 134.3 keV γ ray (top of Fig. 3) shows, on one hand, lines belonging to the A and B bands and, on the other, lines on top of the upper isomer. Among these there is a strong 120.4 keV line ($E1$ because of intensity balance con-

TABLE I. (*Continued*).

E_γ (keV)	I_γ (arb. units)	I_T (arb. units)	Multipolarity	a_2
297.8	38(11)	5(2)	$E2$	
300.8	19(4)	3.0(6)	$M1$	
307.5	24(4)	3.8(7)	$M1$	
311.0	28(4)	4.0(6)	$E2$	
386.1[e]	49(10)[e]	6(1)	$E2$	0.56(14)
386.4[c,e]	29(7)[e]	4(1)	$E2$	
416.5	61(12)	8(1.6)	$E1$	
437.6	18(3)	2.2(4)	$E2$	0.3(1)
447.5	42(8)	5(1)	$E2$	0.7(2)
465.6	19(5)	2.5(7)	$E2$	
474.6	30(5)	3.8(6)	$E2$	0.24(2)
498.7	24(4)	3.0(5)	$E2$	
507.5	30(5)	3.8(6)	$E2$	
514.6	12(4)	1.5(5)	$E2$	
524.4	25(5)	3.2(6)	$E2$	
536.2	25(3)	3.2(4)	$E2$	0.37(7)
539.1	9(2)	1.2(3)	$E2$	
543.9	30(6)	3.8(8)	$E2$	
567.0	25(4)	3.2(5)	$E2$	
583.7	8(1.6)	1.0(2)	$E2$	
597.5	24(5)	3.0(6)	$E2$	0.52(14)
677.5	73(8)	9(1)	$M2$	
724.6	47(8)	6(1)		
760.7	18(4)	2.4(5)		

[a]Energies to within 0.1–0.3 keV.
[b]Contaminated with ^{178}Hf, which has been discounted.
[c]Contaminated with ^{181}Re, which has been discounted.
[d]The symbol D means $a_2 < 0$ but very large uncertainty.
[e]Several energies and intensities have been determined from coincidence spectra.
[f]$(9^-) \rightarrow (8^-)$ transition.
[g]$(14^+) \rightarrow (13^-)$ transition.
[h]Upper limits for intensity.

siderations and fortunately resolved from the lower lying 121.1 keV γ ray) and other transitions (263.3, 276.1, 290.1, and 307.5 keV and the corresponding crossovers) which order themselves as a band (C band).

Singles as well as coincidence intensity considerations suggest that the two low lying 134.3 keV γ rays are most likely $M1$ (for the B band member) and $E2$, and $E1$ for the upper lying. The 121.1 keV γ ray is $E1$ (like the 78.6 keV member), both because of the lifetime of the state it depopulates and because of intensity balance considerations. Its anisotropy being negative leaves us with one unit of spin less for the I of the state at 138.6 keV. The 92.3 keV line is $M1$ or $E2$ (equal internal conversion at this energy), but its negative anisotropy favors $M1/E2$, $\Delta I = 1$, again bringing the spin down one unit.

Moving to the left in Fig. 5, we find a weakly populated band based on the state at 138.6 keV (D band).

Another point to be mentioned is the existence of the 46.3 keV γ ray coming delayed with respect to the rest of the level scheme (in particular, clearly in delayed but not in prompt coincidence with the 121.1 keV line). This establishes an isomeric level (of 66±20 ns) at 46.3 keV on which the rest of the scheme is built (because of intensity balance the 46.3 keV γ ray is most likely $M1$).

Summarizing, we may say that if the spin parity of the effective ground state is I_0^π, the most likely choices for the I^π's of the bandhead states of the A, B, and D bands are $(I_0+3)^\pi$, $(I_0+3)^{-\pi}$, and $(I_0+2)^\pi$, respectively. Moving up through the B and especially the A band, one obtains $(I_0+8)^{-\pi}$ for the isomeric state at 1542.1 keV and, consequently, $(I_0+10)^{-\pi}$ for the bandhead state of the C band.

An additional feature of the level scheme is shown at the far left of Fig. 5, which displays a crossoverless band composed most likely of a $\Delta I = 2$ sequence. Spectra gated by lines of this cascade are shown in Fig. 4. The 191.1 keV gated spectrum is contaminated with the 191.7 keV, $\frac{13}{2}^- \rightarrow \frac{11}{2}^-$ transition of ^{181}Re (Ref. 4). The 297.8 keV gated spectrum is pure, clearly showing the whole cascade and, finally, the 386.4 keV gated spectrum is again contaminated by the 386.0 keV $\frac{21}{2}^- \rightarrow \frac{17}{2}^-$ transition in ^{181}Re (Ref. 4) and the 386.1 keV crossover in ^{180}Re.

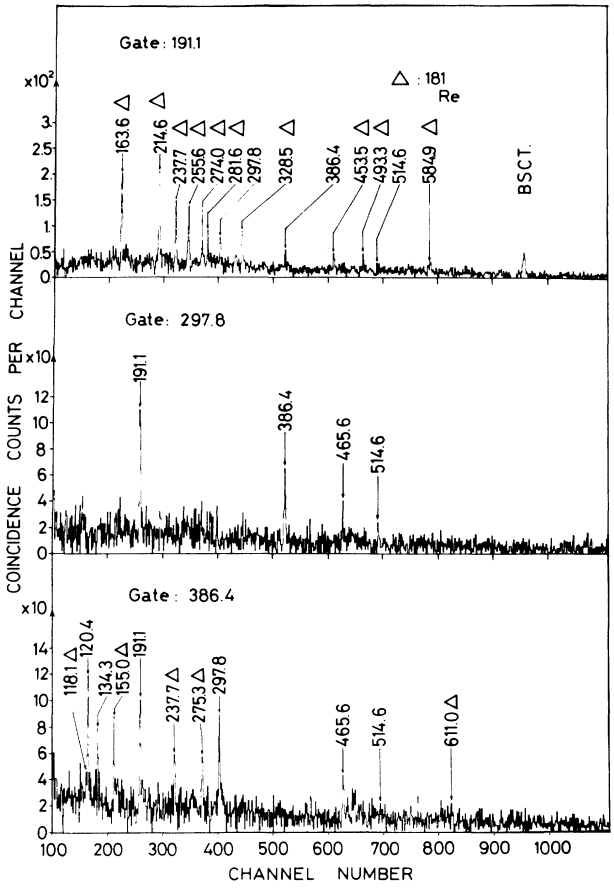

FIG. 4. Coincidence spectra gated by the 191.1, 297.8, and 386.4 keV transitions. The 191.1 and 386.4 keV gates are contaminated by lines of ^{181}Re. BSCT indicates a backscattering effect.

The spin-parity assignments in this band are tentatively made on purely theoretical grounds to be discussed below. Table II gives the quantitative evaluation of coincidence intensity data for this last band to illustrate the general procedure.

IV. STRUCTURE OF THE LEVELS

A first approximation to the excitation spectra of deformed odd-odd nuclei can be obtained by coupling single-quasiproton and quasineutron states of neighboring odd-mass nuclei. This coupling is normally additive for excitation energy as well as for the projection quantum number K. (Exceptions to this rule appear when decoupled states are involved;[6] see below.) Each pair of states characterized by Ω_p and Ω_n produces two in the doubly odd spectrum, namely $K_{\gtrless} = |\Omega_p \pm \Omega_n|$. These two states are possibly split by the residual proton-neutron (p-n) force according to the Gallagher-Moszkowski coupling rules.[7]

Figures 6, 7, and 8 show the systematics of single quasiparticle states in neighboring odd Z, Re and odd N, W and Os isotopes, respectively. Only states of up to approximately 500 keV have been included. Particlelike (holelike) excitations are drawn as having positive (negative) energies.

The quasiparticle energies corresponding to ^{180}Re ($N=105$, $Z=75$) have been obtained by linear interpolation of the values of neighboring odd mass nuclei. The proton single particle level energies are obtained from ^{179}Re ($N=104$) and ^{181}Re ($N=106$) and the neutron ones from ^{179}W ($Z=74$) and ^{181}Os ($Z=76$). Using these values a zero order level scheme for ^{180}Re can be constructed. Table III shows the results of such a procedure in the form of a matrix whose axes are the p and n states. Each entry gives the two values $K_{\gtrless} = |\Omega_n \pm \Omega_p|$ (the one underlined corresponds to the state with proton and neutron intrinsic spins aligned) and the zero order energy (no p-n interaction considered).

The predicted ground state is a 1^- state. This coincides with the data[2] known from radioactive decay studies. This ^{180}Re^g isomer has, in fact, been classified[8] as the aligned coupling of the Nilsson orbitals $\pi\frac{5}{2}^+[402]$ and $\nu\frac{7}{2}^-[514]$, while a 1^+ state, at 20 keV, is describable[8] as $\pi\frac{9}{2}^-[514]+\nu\frac{7}{2}^-[514]$ (also aligned coupling). The energy of the 1^+ level is found to be much lower than predicted (see Table III). This shows that shifts in excitation energies of about 150 keV, with respect to estimates, can easily be expected. This also coincides with an average value for the Gallagher-Moszkowski splitting.[7,17]

How can we proceed now in front of a complex level scheme in which the spin parity of its "effective" ground state is unknown? The key to an understanding of the structure of the ^{180}Re (and other deformed doubly odd nuclei as well) is the examination of its band structure. There are two quantities attached to a band which we shall exploit to characterize a given structure. One is the K value and the other is the moment of inertia $\mathcal{I}/\hbar^2$

TABLE II. Total transition coincidence intensities[a] for the $\Delta I=2$ cascade.

Gating energy (keV)	Displayed energy (keV)				
	191.1	297.8	386.4	465.6	514.6
191.1		7.3(9)	5.6(8)	3.7(9)	2.3(6)
297.8	14.5(15)		8(1)	5.7(9)	4.9(9)
386.4	11(1)	11(1)		7.9(15)	5.0(15)

[a]Assumed multipolarity is $E2$.

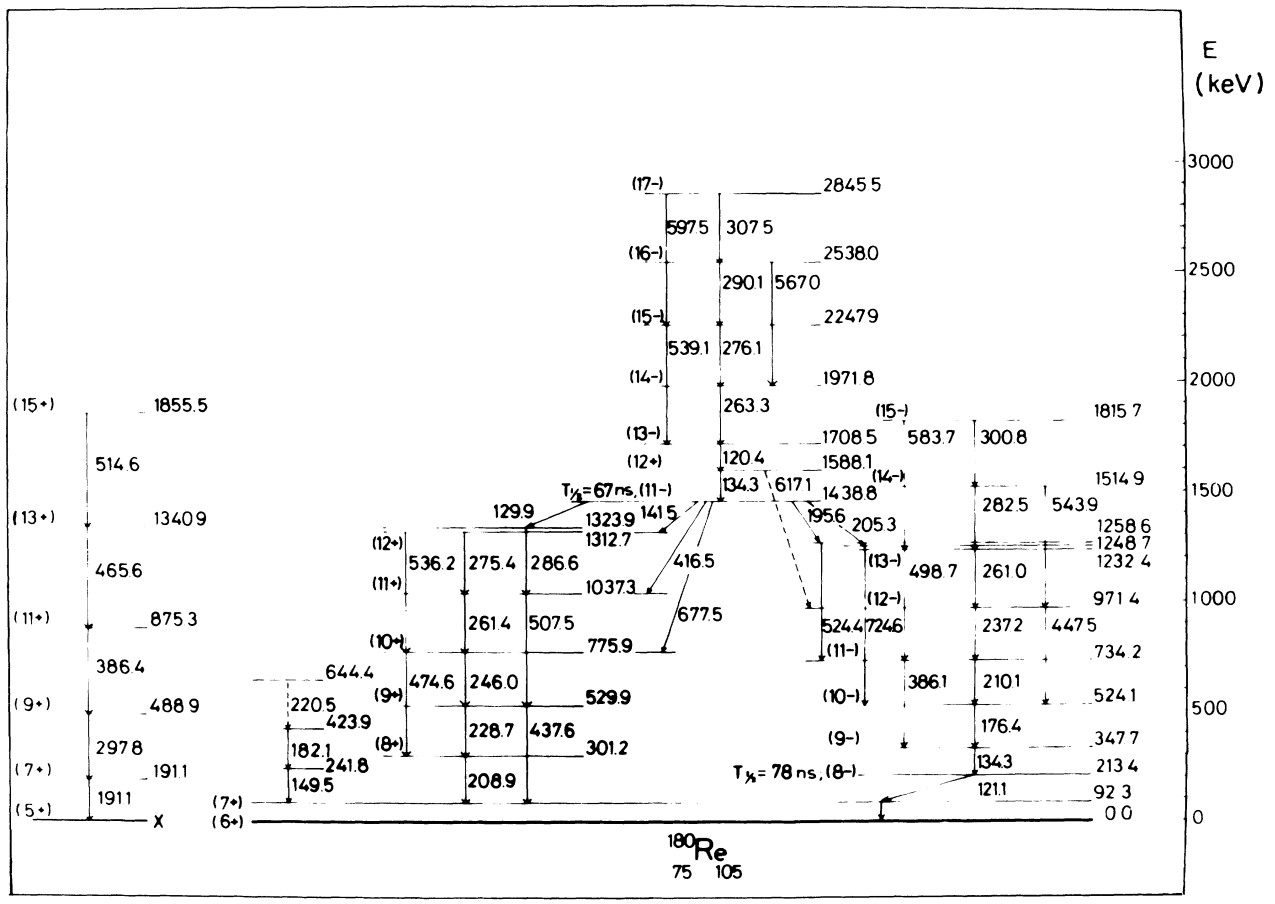

FIG. 5. Proposed level scheme for ^{180}Re. Excitation energies are referred to the (5^+) "effective" ground state. The band shown at the far left of the figure does not show any connection with the rest of the scheme; its excitation energy is unknown.

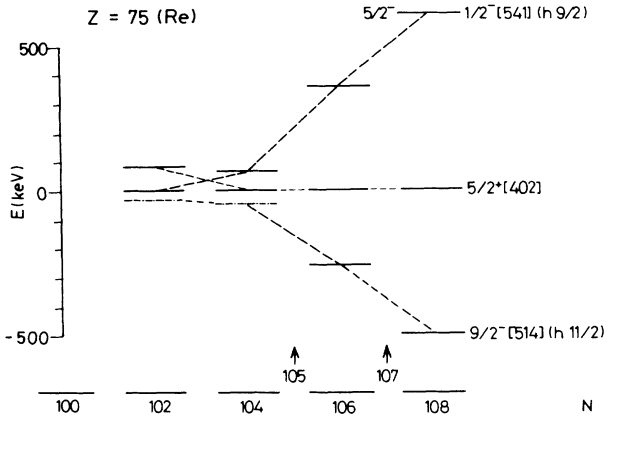

FIG. 6. Neutron number (N) dependence of proton single-quasiparticle levels in odd Re isotopes (Refs. 2, 4, and 13). Horizontal dashed lines are levels of uncertain excitation energy.

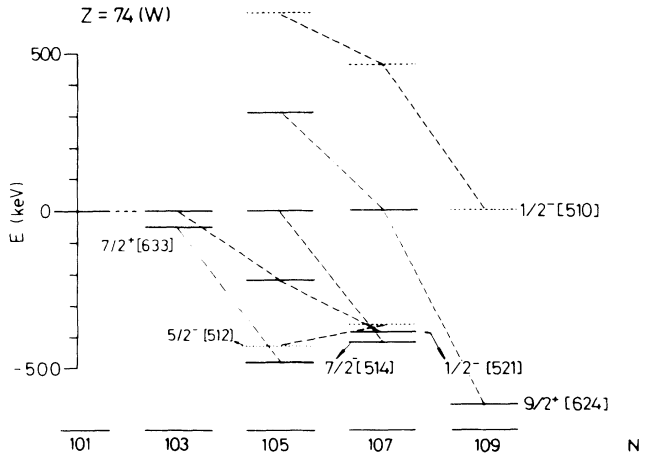

FIG. 7. Neutron number dependence of neutron single quasiparticle levels in odd W isotopes (Refs. 2 and 14).

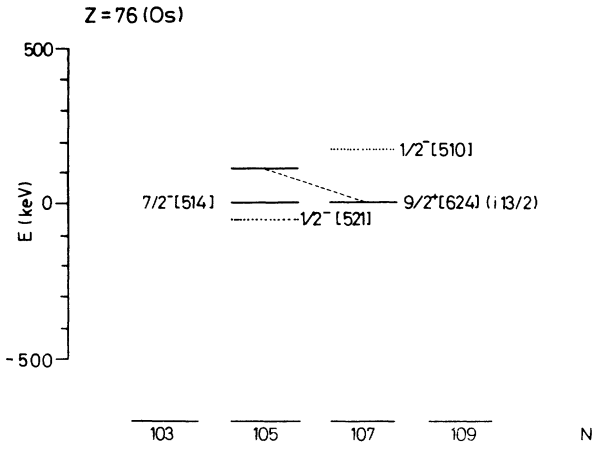

FIG. 8. Neutron number dependence of neutron single quasiparticle levels in odd Os isotopes (Ref. 2).

(measured in units of MeV^{-1}).

For a band of constant $\mathcal{I}$ and given K, the ratio x of the first two consecutive transition energies is $(K+2)/(K+1)$. For large K values, x approaches 1 monotonically and its value is 2 for $K=0$. This expression can be inverted to give $K=(2-x)/(x-1)$ (this quantity shall be denoted K_1). On the other hand, if K is known, it is possible to extract the moment of inertia from just the first transition energy through

$$\mathcal{I}^{(1)}/\hbar^2=(K+1)/[E(K+1)-E(K)] .$$

This procedure works well for intrinsic excitations ($K\neq\frac{1}{2}$) with negligible Coriolis mixing, as can be seen in Table IV, where K and $\mathcal{I}$ have been extracted for bands in neighboring odd-mass nuclei.[2]

As an example, let us discuss the $\tilde{\pi}\frac{9}{2}^-[514]$ band[2] in ^{179}Re. We get $K_1=4.75$ and $\mathcal{I}^{(1)}/\hbar^2=33.23\ \mathrm{MeV}^{-1}$ (see Table IV). For this kind of band, which we shall call *normal*, K_1 is usually slightly larger than K because the moment of inertia increases with I. [For instance, if we calculate the energy of the second transition, $E(K+2)-E(K+1)$, using $\mathcal{I}^{(1)}/\hbar^2$ we get 195.6 versus 194.3 keV measured.[2]] The nonrigidity can be taken into account, but for the moment, to keep the discussion as simple as possible, it is neglected.

There are, however, other types of bands for which this procedure fails. In odd neutron nuclei (W and Os) we find $\frac{1}{2}^-[521]$ and strongly Coriolis *distorted* $\frac{9}{2}^+[624]$ ($i_{13/2}$ parentage) bands. Signature[9] dependent effects related to significant decoupling parameters split these bands into two $\Delta I=2$ sequences [the signature may be defined as $(-1)^I$]. In odd proton nuclei (Re), on the other hand, one finds decoupled[10] $\frac{1}{2}^-[541]$ ($h_{9/2}$ parentage[1]) bands. Hence, one may try to apply similar procedures to those discussed above for $\Delta I=1$ bands, but now for the $\Delta I=2$ cascades.

A K value (denoted K_2) is obtained in this case from the ratio

$$[E(K+4)-E(K+2)]/[E(K+2)-E(K)] =(2K+7)/(2K+3) ,$$

of the two lowest $\Delta I=2$ transitions through $K_2=\frac{1}{2}(7-3x)/(x-1)$. A moment of inertia is calculated using

TABLE III. Zeroth-order approximation to the spectrum of ^{180}Re.[a]

$\tilde{\nu}\Omega^{\pi}[Nn_3\Lambda]$	$\tilde{\pi}\Omega^{\pi}[Nn_3\Lambda]=\frac{5}{2}^+[402]$			
E (MeV)	E (MeV)	0	$\frac{9}{2}^-[514]$ $\simeq 0.156^{d}$	$\frac{5}{2}^-(\frac{1}{2}^-[541])$ 0.211
$\frac{7}{2}^-[514]$		$\underline{1}^-,6^-$	$\underline{1}^+,8^+$	$\underline{3}^+,4^+$
0		0	0.156	0.211
$\frac{1}{2}^-[521]^{b}$		$\underline{2}^-,3^-$	$\underline{4}^+,5^+$	$\simeq 5^+$
$\simeq 0.136$		0.136	0.292	0.347
$\frac{9}{2}^+[624]$		$2^+,\underline{7}^+$	$0^-,\underline{9}^-$	$\underline{4}^-,5^-$
0.208		0.208	0.364	0.419
$\frac{5}{2}^-[512]^{c}$		$0^-,\underline{5}^-$	$2^+,\underline{7}^+$	$\underline{2}^+,3^+$
$\frac{7}{2}^+[633]^{c}$		$1^+,\underline{6}^+$	$1^-,\underline{8}^-$	$\underline{3}^-,4^-$

[a]Each entry in the table gives the two possible values $K^{\pi}_{\gtrless},K_{\gtrless}=|\Omega_{\pi}\pm\Omega_{\nu}|$ and the excitation energy of the state. The one underlined corresponds to the state with proton and neutron intrinsic spins aligned.

[b]The energy of this orbital has been taken as zero in ^{181}Os.

[c]Since the $\frac{5}{2}^-[512]$ and $\frac{7}{2}^+[633]$ orbitals are unknown in ^{181}Os, the interpolation procedure described in the text cannot be used and these excitation energies remain undetermined.

[d]This is a lower limit for the energy of the $\frac{9}{2}^-[514]$ orbital since its exact position in ^{179}Re is unknown.

TABLE IV. K values and moments of inertia (see text) extracted from bands in $A \simeq 180$ odd-mass and even-even nuclei (Ref. 2).

Nucleus	$\Omega^{\pi}[Nn_3\Lambda]$	K_1	K_2	$\mathcal{J}/\hbar^2$ (MeV^{-1})	$\delta\mathcal{J}/\hbar^2$ (MeV^{-1})
^{179}Re	$\frac{5}{2}^+[402]$	2.89		28.27	−0.06
	$\frac{1}{2}^-[541]$		1.38[b]	34.16[c]	5.83
	$\frac{9}{2}^-[514]$	4.75		33.23	4.90
^{181}Re	$\frac{5}{2}^+[402]$	2.87		29.64	0.70
	$\frac{1}{2}^-[541]$		1.10[b]	33.36[c]	4.42
	$\frac{9}{2}^-[514]$	5.00		33.48	4.54
^{183}Re	$\frac{5}{2}^+[402]$	2.70		30.58	0.61
	$\frac{1}{2}^-[541]$		0.81[b]	32.71[c]	2.74
	$\frac{9}{2}^-[514]$	4.74		32.80	2.83
^{179}W	$\frac{7}{2}^-[514]$	3.84		37.52	9.19
	$\frac{7}{2}^+[633]$[a]				
	$\frac{9}{2}^+[624]$	1.00	1.16	33.29[c]	4.96
	$\frac{5}{2}^-[512]$			34.57	6.24
	$\frac{1}{2}^-[521]$		0.13[b]	33.76[c]	5.43
^{181}W	$\frac{7}{2}^-[514]$	3.39		37.72	8.78
	$\frac{9}{2}^+[624]$	3.62	3.67	41.15[c]	12.21
^{181}Os	$\frac{7}{2}^-[514]$	3.96		36.44	13.68
	$\frac{9}{2}^+[624]$	−0.01	1.63	28.09[c]	5.33
	$\frac{1}{2}^-[521]$		0.09[b]	31.03[c]	8.27
^{183}Os	$\frac{9}{2}^+[624]$	2.64	2.76	38.83[c]	15.23
^{178}W	0^+			28.33	
^{180}W	0^+			28.94	
^{182}W	0^+			29.97	
^{180}Os	0^+			22.76	
^{182}Os	0^+			23.60	

[a]No reliable parameters can be extracted for this very distorted structure (Ref. 2).
[b]This quantity is R_0 (see text).
[c]Corresponds to $\mathcal{J}^{(2)}/\hbar^2$ (see text).

$$\mathcal{J}^{(2)}/\hbar^2=(2K_2+3)/[E(K+2)-E(K)] .$$

(For the $\frac{1}{2}^-[541]$ proton and $\frac{1}{2}^-[521]$ neutron decoupled bands,[1] $K2$ coincides with the value R_0 defined below. For these bands R, the collective spin, rather than K, is the good quantum number.) The distorted $\frac{9}{2}^+[624]$ bands have transition energies which are quite compressed, as compared to a normal situation due to strong Coriolis mixing, giving small K_2 values which reflect the admixture to other orbitals with lower K. (If K would be used to calculate $\mathcal{J}^{(2)}$, one would obtain unreasonably large values.) Table IV, column 6, also lists the deviation of the moment of inertia in a given odd-mass nucleus with respect to $\mathcal{J}$ in the core nucleus, which has one proton or one neutron less [$\mathcal{J}$ is obtained in the even-even cores through $3/E(2^+)$].

We must now combine the information on odd protons and neutrons in order to understand the structure of doubly odd nuclei. As we shall see, a wealth of different coupling schemes will appear.

The most simple one is the combination of two normal bands which gives again a normal behavior [it follows the $I(I+1)$ law]. In this case we expect additivity in both K_1 ($K_1=K_{1,\pi}+K_{1,\nu}$) and $\mathcal{J}^{(1)}$ [i.e., $\mathcal{J}^{(1)}$(odd-odd)$=\mathcal{J}$(even-even)$+\delta\mathcal{J}^{(1)}$(odd π)$+\delta\mathcal{J}^{(1)}$(odd ν); with $\delta\mathcal{J}^{(1)}$(odd π,ν)$=\mathcal{J}^{(1)}$(odd π,ν)$-\mathcal{J}$(even-even)]. We shall adopt the following association: To describe ^{180}Re we take values from ^{179}Re, ^{179}W, and ^{178}W. Other, more so-

TABLE V. Experimental and calculated K values and moments of inertia for ^{180,182}Re (Ref. 3).

Nucleus	I^π	K_1	K_2	Identification π	Identification ν	K^{calc}	$\mathcal{J}^{expt}/\hbar^2$ (MeV^{-1})	$\mathcal{J}^{calc}/\hbar^2$ (MeV^{-1})
^{180}Re	(6^+)	0.61	1.51	$\frac{5}{2}^+[402]+\frac{7}{2}^+[633]$				
	(7^+)	3.59		$\frac{5}{2}^+[402]+\frac{9}{2}^+[624]$		3.89	30.70[a]	33.23
	(8^+)	9.55		$\frac{9}{2}^-[514]+\frac{7}{2}^-[514]$		8.59	43.08	42.42
	(8^-)	2.19	3.06	$\frac{9}{2}^-[514]+\frac{7}{2}^+[633]$			29.35[b]	
	(9^-)	4.23	5.36	$\frac{9}{2}^-[514]+\frac{9}{2}^+[624]$		5.91	35.53[b]	38.19
	(13^-)			$\frac{9}{2}^-[514]+(\frac{7}{2}^-[514]$ $+\frac{1}{2}^-[521]+\frac{9}{2}^+[624])$		9.72		52.81
	(15^-)	19.57	16.96	$\frac{9}{2}^-[514]+(\frac{7}{2}^-[514]$ $+\frac{5}{2}^-[512]+\frac{9}{2}^+[624])$		13.21	60.77	53.62
	(5^+)		2.08	$\frac{1}{2}^-[541]+\frac{1}{2}^-[521]$		1.51	37.49[c]	39.59
^{182}Re	7^+	3.94	4.64	$\frac{5}{2}^+[402]+\frac{9}{2}^+[624]$		6.54	36.17[b]	41.85
	9^-	5.61	6.12	$\frac{9}{2}^-[541]+\frac{9}{2}^+[624]$		8.62	38.97[b]	45.69
	2^+	1.69	1.67	$\frac{5}{2}^+[402]-\frac{9}{2}^+[624]$		0.75	48.07[b]	41.85
	4^-	1.92	2.06	$\frac{1}{2}^-[541]-\frac{9}{2}^+[624]$		2.52	38.10[b]	45.57

[a]Corresponds to $(2K_1+3)/[E(K+2)-E(K)]$ since K_2 cannot be calculated.
[b]Corresponds to $\mathcal{J}^{(2)}/\hbar^2$ (see text).
[c]Corresponds to $(2R_0+3)/[E(R_0+2)-E(R_0)]$.

phisticated, procedures can be imagined (like various averagings), but the results are qualitatively similar. From Table III we see that a good candidate for such a structure is the low lying 8^+, $\tilde{\pi}\frac{9}{2}^-[514]+\tilde{\nu}\frac{7}{2}^-[514]$ state. Among the low lying bands in ^{180}Re the most normal "looking" is the A band. (The difference between consecutive transition energies, a quantity related to the inverse of the moment of inertia, stays, relatively speaking, more constant in this band than in others.) By the procedures described above, one obtains $K_1=9.55$ versus a calculated value of 8.59 (see Table V). If one assumes $K=8$, $\mathcal{J}^{(1)}/\hbar^2$ has the value 43.08 versus 42.42 MeV^{-1} calculated (from the data in Table IV), giving a striking agreement. With the experimental value of $\mathcal{J}^{(1)}$ one obtains 232.1 versus 228.7 keV for the second cascade transition.

Once a single spin parity is adopted, the rest of the assignments follow, as discussed in the preceding sections. For instance, the D bandhead state (at 138.6 keV) has $I^\pi=(7^+)$. It is interesting to note that the transition energies of this weakly populated band are similar to the ones in the 7^+ band reported in ^{182}Re (Ref. 3) (namely 154.1 and 185.3 keV) and interpreted as based on the $\tilde{\pi}\frac{5}{2}^+[402]+\tilde{\nu}\frac{9}{2}^+[624]$ configuration. In fact, as seen from Table III, this configuration lies quite low in energy and its inversion with respect to the 8^+ $(\tilde{\pi}\frac{9}{2}^-[514]+\tilde{\nu}\frac{7}{2}^-[514])$ band may be due to the p-n force since its intrinsic spins are aligned. Table V shows that the extracted K_1 (K_2 cannot be calculated because of a lack of sufficient information) is significantly lower than 7. This is certainly related to the presence of the $\frac{9}{2}^+[624]$ neutron in its structure. As already discussed, the neutron band labeled $\frac{9}{2}^+[624]$ (Ref. 2) is strongly distorted due to Coriolis admixtures, primarily with the $\frac{7}{2}^+[633]$ orbital, which is much lower in ^{179}W than in ^{181}W. [These bands are complicated because the collective and intrinsic energies are not separated, they do not follow the $I(I+1)$ law, and the intrinsic state changes rapidly along the band; the extraction of parameters from these bands is not reliable.] This circumstance will cause a strong mixing between the $K^\pi=7^+$ $(\tilde{\pi}\frac{5}{2}^+[402]+\tilde{\nu}\frac{9}{2}^+[624])$ and $K^\pi=6^+$ $(\tilde{\pi}\frac{5}{2}^+[402]+\tilde{\nu}\frac{7}{2}^+[633])$ configurations, bringing the 7^+ band energies down with respect to their unperturbed positions. It may even be that the 6^+ state at 46.3 keV and, consequently, the 92.3 keV transition belong to this system of states. The fact that the 6^+ state cannot be affected by the above mentioned mixing may explain the smallness of the 92.3 keV transition energy as compared to 149.5 keV. A similar situation seems to repeat itself in the B band. As already mentioned, the portion of this band starting at 394.0 keV is very similar to the $I^\pi=9^-$ band in ^{182}Re (Ref. 3). Again here, the two configurations, $K^\pi=8^-$ $(\tilde{\pi}\frac{9}{2}^-[514]+\tilde{\nu}\frac{7}{2}^+[633])$ and $K^\pi=9^-$ $(\tilde{\pi}\frac{9}{2}^-[514]+\tilde{\nu}\frac{9}{2}^+[624])$, must be strongly admixed and the $(9^-)\rightarrow(8^-)$ transition (134.3 keV) is smaller than one would expect from the $(10^-)\rightarrow(9^-)$ transition. Table V also shows that for this case both the K_1 and K_2 values are much smaller than K. We may call this kind of distortion compression, and we note that the additivity properties of K and $\mathcal{J}$ are not so well fulfilled (see also ^{182}Re in Table V). This is a coupling involving a particle (in this case a proton) which is strongly attached to the symmetry axis and another which tends to decouple. This kind of structure is different from the one called semidecoupled[1,11,12] in which one of the particles is com-

pletely decoupled and the other is like the neutron in the previous case (i.e., a high j particle in an orbit with K significantly larger than $\frac{1}{2}$). In this last case the Coriolis staggering of the nondecoupled particle is transmitted to the semidecoupled band in the odd-odd nucleus while the other particle is more or less an inert spectator.

We turn now to the high lying isomer at 1542.1 keV, which most likely has $I^{\pi}=13^{-}$. With this spin value it has to be a four-quasiparticle state and its excitation energy is consistent with the energy required to break a pair in a blocked system. A good candidate for its configuration is $\tilde{\pi}\frac{9}{2}^{-}[514]+\tilde{\nu}(\frac{7}{2}^{-}[514]+\frac{1}{2}^{-}[521]+\frac{9}{2}^{+}[624])$, $K^{\pi}=13^{-}$. We may visualize this as the coupling of the 8^{-} band to a pair of neutrons originally from the $\frac{1}{2}^{-}[521]$ level (this orbit is the lowest below the Fermi surface as can be seen in Figs. 7 and 8), where one of them jumps into the $\frac{9}{2}^{+}[624]$ orbit (first above the Fermi level).

The C bandhead state has most likely $I^{\pi}=15^{-}$, which can be understood in a similar way as $\tilde{\pi}\frac{9}{2}^{-}[514]+\tilde{\nu}(\frac{7}{2}^{-}[514]+\frac{5}{2}^{-}[512]+\frac{9}{2}^{+}[624])$, $K^{\pi}=15^{-}$ (the $\frac{5}{2}^{-}[512]$ is the second lowest below the Fermi surface). If this is accepted, and $\mathcal{I}$ is calculated from the first transition of 263.3 keV, the second transition is calculated to be 279.7 versus 276.1 keV measured. In spite of the assumed participation in this structure of the $\frac{9}{2}^{+}[624]$ neutron, its behavior is rather normal. The calculated K_1 and K_2 values are fairly high. The value of $\mathcal{I}^{(1)}$ (see Table V) is $\approx$2.15 times larger than $\mathcal{I}$ of the core nucleus ^{178}W, which may be due principally to reduced pairing and perhaps larger deformation. The reduced pairing may contribute significantly to reduce the coupling between the $\frac{9}{2}^{+}[624]$ (above Fermi level) to the lower K components of the $i_{13/2}$ parentage Nilsson multiplet (below Fermi level). Certainly, here, additivity is not expected since the building blocks cannot reflect the structural changes occurring in the composite system.

The last feature to be discussed is the possible structure of the (5^{+}), $\Delta I=2$ band. We suggest that it is the analog of the double decoupled structure reported in $^{182-186}$Ir (Ref. 1) built from the decoupled $\frac{9}{2}^{-}$ proton band ($\frac{1}{2}^{-}[541]$ as the main component) and the $\frac{1}{2}^{-}[521]$ neutron (which generates highly distorted $\Omega_n=\frac{1}{2}$ bands because of its decoupling parameter near unity). Angular momenta are added here along a direction perpendicular to the symmetry axis (the R direction), while K values are essentially zero. The additivity for R_0 (see below) and $\mathcal{I}$ holds well in this case (see Table V).

In order to further explore this possibility, an analysis of alignments[9,1] has been made. The alignment i has been extracted for the $h_{9/2}$ band in ^{179}Re (Ref. 13), the $\frac{1}{2}^{-}[521]$ band in ^{179}W (Ref. 14), and the $\Delta I=2$ band in ^{180}Re (under the assumption of $I^{\pi}=5^{+}$ for the bandhead state) by referring all three of these structures to the ground state band of ^{178}W. The collective angular momentum $R+\frac{1}{2}$ in this ground state band is represented by $R+\frac{1}{2}=(\mathcal{I}_0+\mathcal{I}_1\omega^2)\omega$, with $\mathcal{I}_0/\hbar^2=27.9$ MeV^{-1} and $\mathcal{I}_1/\hbar^4=111.0$ MeV^{-3}. (Here the rigid rotor simplification has been dropped.)

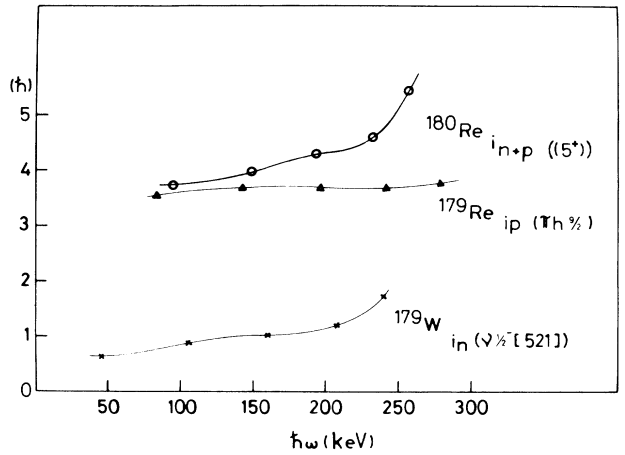

FIG. 9. Alignment i (in units of $\hbar$) as a function of rotational frequency ($\hbar\omega$) for three $\Delta I=2$ sequences in ^{179}W($\frac{1}{2}^{-}[521]$), ^{179}Re($h_{9/2}(\frac{1}{2}^{-}[541])$), and ^{180}Re.

The alignment for the odd and doubly odd nuclei is then obtained by subtracting from the component of the total angular momentum along the rotation axis, $I_x=[(I+\frac{1}{2})^2-K^2]^{1/2}$, the collective contribution, namely $i=I_x-(R+\frac{1}{2})$.

Figure 9 shows the results of such an analysis. One may say that the relation

$$i_{n+p}(5^{+})=i_n(\tfrac{1}{2}^{-}[521])+i_p(h_{9/2})$$

is fulfilled only in a qualitative way. The alignment in the ^{180}Re (5^{+}) band is somewhat larger than in the $h_{9/2}$ band (but less than i_n+i_p), while the frequency dependence resembles that for the $\frac{1}{2}^{-}[521]$ band in ^{179}W.

The $\Delta I=2$ character of this band can be supported by an analysis of the same kind as that performed in Ref. 1 for ^{186}Ir. The energy spacings along this band are typical of $\Delta I=2$ transitions (comparable to those of the

TABLE VI. Experimental and calculated ratios $R_I=(E_I-E_5)/(E_7-E_5)$ and $R_I=E_I/E_{2^+}$ for the (5^{+}) band and the ground state band in ^{180}Re and ^{178}W, respectively (see text).

	^{180}Re			^{178}W	
I	R_I^{expt}	R_I^{calc}	I	R_I^{expt}	R_I^{calc}
11	4.58	4.68	6	6.55	7.00
13	7.02	7.35	8	10.77	12.00
15	9.71	10.58	10	15.71	18.33

TABLE VII. Different coupling schemes in a deformed doubly odd nucleus.

Neutron \ Proton	normal, pure K, $\Delta I=1$	Coriolis distorted, high j, $\Delta I=1$, staggered	decoupled, $\Delta I=2$
normal, pure K, $\Delta I=1$	normal, pure K, $\Delta I=1$	compressed, $\Delta I=1$	nondistorted,[a] $\Delta I=1$
Coriolis distorted, high j, $\Delta I=1$, staggered		compressed, $\Delta I=1$	semidecoupled,[b] $\Delta I=1$, staggered
decoupled, $\Delta I=2$			doubly decoupled, $\Delta I=2$

[a]The transition energies in the doubly odd nucleus resemble the ones in the normal band of the odd nucleus. The decoupled particle acts as a spectator.
[b]See Refs. 11 and 12.

crossover transitions in the $\Delta I=1$ bands) and cannot be reproduced to any acceptable precision by a $\Delta I=1$ structure. These energy spacings increase very rapidly, in sharp contrast to the slow increment in transition energy along the $\Delta I=1$ bands in this nucleus (typical of high K bands).

We assume that the (5^+) state has $R_0\neq 0$ for the expectation value of the collective angular momentum, which increases in steps of two units along the band and that the level energies follow an $R(R+1)$ law. R_0 and the rotational constant $A=\hbar^2/2\mathcal{J}$ can be deduced from the two first transition energies and used, in turn, to predict the upper ones. One obtains $R_0=2.08\ \hbar$ and $A=13.34$ keV (compare with Table V). The predicted ratios $R_I=(E_I-E_5)/(E_7-E_5)$ are compared to the experimental values in Table VI and the agreement is suggestive. Similar ratios are also given for ^{178}W, showing a larger deviation from the asymptotic limit than the values for ^{180}Re.

These results (and general theoretical considerations, more fully explained in Ref. 1, about the conditions for appearance of $\Delta I=2$ bands in odd-odd nuclei) form the basis for the present interpretation. This subject is being further explored in more neutron deficient Re isotopes, where the double decoupled structure should come very close to the ground state on account of the neutron number variation of proton and neutron quasiparticle levels.

Table VII gives a summary of the different coupling schemes and their main features discussed in the present section.

V. CONCLUSIONS

A completely new high-spin level scheme has been obtained for ^{180}Re comprising essentially five rotational sequences.

A good description has been obtained for the low-lying intrinsic states resorting to the available single-quasiparticle information in neighboring odd proton and neutron nuclei.

In particular, a crossover free cascade is tentatively interpreted as a new example of a double decoupled band originally described in $^{182-186}$Ir.

The different coupling schemes which may arise in a deformed doubly odd nucleus are discussed. For normal (pure K, $\Delta I=1$) and doubly decoupled ($\Delta I=2$) structures a good additivity is found for K (or R_0) and $\mathcal{J}$. They follow, respectively, the $I(I+1)$ or $R(R+1)$ laws. The other intermediate cases are more irregular and do not respond to such simple rules.

Note added. In fact, these structures have also been detected[15] in ^{176,178}Re during the revision of the present work. Also in the process of revision, we learned about another investigation concerning ^{180}Re (Ref. 16). The main disagreement is that these authors base their scheme on the known $(2)^+$ state[2] at 74.6 keV, something which is incompatible with our results.

ACKNOWLEDGMENTS

This work was supported in part by the Consejo Nacional de Investigaciones Científicas y Técnicas, Argentina, and the U.S. National Science Foundation under Contract No. INT-81-19006.

[1]A. J. Kreiner, D. E. Di Gregorio, A. J. Fendrik, J. Davidson, and M. Davidson, Phys. Rev. C **29**, 1572 (1984); Nucl. Phys. **A432**, 451 (1985); A. J. Kreiner, P. Thieberger, and E. Warburton, Phys. Rev. C **34**, 1150 (1986), and references therein.
[2]*Table of Isotopes,* edited by C. M. Lederer and V. S. Shirley (Wiley, New York, 1978).
[3]M. F. Slaughter, R. A. Warner, T. L. Khoo, W. H. Kelly, and W. C. McHarris, Phys. Rev. C **29**, 114 (1984).
[4]A. Neskakis, R. M. Lieder, M. Müller-Veggian, H. Beuscher, W. F. Davidson, and C. Mayer-Böricke, Nucl. Phys. **A126**,

189 (1976).
[5]F. Dubbers, L. Funke, P. Kemnitz, K. D. Schilling, H. Strusny, E. Will, G. Winter, and M. K. Balodis, Nucl. Phys. **A315**, 317 (1979).
[6]A. J. Kreiner, C. Alonso Arias, M. Debray, D. Di Gregorio, A. Pacheco, J. Davidson, and M. Davidson, Nucl. Phys. **A425**, 397 (1984).
[7]C. J. Gallagher and S. A. Moszkowski, Phys. Rev. **111**, 1282 (1958).
[8]B. Harmatz and T. H. Handley, Nucl. Phys. **A121**, 481 (1968).
[9]R. Bengtsson and S. Frauendorf, Nucl. Phys. **A314**, 27 (1979); **A327**, 139 (1979), and references therein.
[10]F. S. Stephens, Rev. Mod. Phys. **47**, 43 (1975).
[11]A. J. Kreiner, M. Fenzl, S. Lunardi, and M. A. J. Mariscotti, Nucl. Phys. **A282**, 243 (1977).
[12]A. J. Kreiner, Z. Phys. A **288**, 373 (1978).
[13]J. R. Leigh, J. O. Newton, L. A. Ellis, M. C. Evans, and M. J. Emmott, Nucl. Phys. **A183**, 177 (1972).
[14]B. J. Meijer, J. Konijn, B. Klank, J. H. Jett, and R. A. Ristinen, Z. Phys. A **275**, 79 (1975); F. M. Bernthal and R. A. Warner, Phys. Rev. C **11**, 188 (1975); Th. Lindblad, H. Ryde, and P. Kleinheinz, Nucl. Phys. **A201**, 369 (1973).
[15]J. Davidson, M. Davidson, M. Debray, G. Falcone, D. Hojman, A. J. Kreiner, I. Mayans, C. Pomar, and D. Santos, Z. Phys. A **324**, 363 (1986).
[16]Ts. Venkova *et al.*, Progress Report of the Hahn Meitner Institut, 1985, p. 160 (unpublished).
[17]J. P. Boisson, R. Piepenbring, and W. Ogle, Phys. Rep. **26c**, 99 (1976).